THE JOURNAL OF BIOLOGICAL CHEMISTRY
Vol. 276, No. 7, Issue of February 16, pp. 4853–4862, 2001
Printed in U.S.A.

FPRP, a Major, Highly Stoichiometric, Highly Specific CD81- and CD9-associated Protein*

Received for publication, October 29, 2000
Published, JBC Papers in Press, November 21, 2000, DOI 10.1074/jbc.M009859200

Christopher S. Stipp‡, David Orlicky§, and Martin E. Hemler‡¶

From the ‡Dana-Farber Cancer Institute and the Department of Pathology, Harvard Medical School, Boston, Massachusetts 02115 and the §Department of Pathology and the University of Colorado Cancer Center, University of Colorado Health Sciences Center, Denver, Colorado 80262

CD81 and CD9, members of the transmembrane-4 superfamily (TM4SF; tetraspanins), form extensive complexes with other TM4SF proteins, integrins, and other proteins, especially in mild detergents. In moderately stringent Brij 96 lysis conditions, CD81 and CD9 complexes are virtually identical to each other, but clearly distinct from other TM4SF complexes. One of the most prominent proteins within CD81 and CD9 complexes is identified here as FPRP, the 133-kDa prostaglandin $F_{2\alpha}$ receptor regulatory protein. FPRP, a cell-surface Ig superfamily protein, associates specifically with CD81 or with CD81 and CD9, but not with integrins or other TM4SF proteins. In contrast to other CD81- and CD9-associating proteins, FPRP associates at very high stoichiometry, with essentially 100% of cell-surface FPRP on 293 cells being CD81- and CD9-associated. Also, CD81·CD9·FPRP complexes have a discrete size (<4 × 10^6 Da) as measured by gel permeation chromatography and remain intact after disruption of cholesterol-rich membrane microdomains by methyl-β-cyclodextrin. Although CD81 associated with both α_3 integrin and FPRP in 293 cells, the $\alpha_3\beta_1$·CD81 and CD81·CD9·FPRP complexes were distinct, as determined by immunoprecipitation and immunodepletion experiments. In conclusion, our data affirm the existence of distinct TM4SF complexes with unique compositions and specifically characterize FPRP as the most robust, highly stoichiometric CD81- and/or CD9-associated protein yet described.

CD81, a member of the transmembrane-4 superfamily (TM4SF),[1] also called tetraspanins, was first identified as the target of an antibody that inhibited proliferation of a B lymphoma cell line (1). Subsequently, it has been implicated in B cell signaling and activation (2), thymus functions (3), T cell co-stimulation (4), myoblast fusion and myotube maintenance (5), and neurite outgrowth (6) and as a receptor for hepatitis C virus (7). Knockout of CD81 in mouse confirmed that it has a role in B cell signaling and activation (8, 9) and in regulation of T cell proliferation (10). Another tetraspanin protein, CD9, was identified first as a lymphohemopoietic marker (11) and later was implicated in cell motility (12), metastasis (13), heparin-binding epidermal growth factor activity (14), neurite outgrowth (15), myotube formation and maintenance (5), and sperm-egg binding and fusion (16). Consistent with this, knockout of mouse CD9 caused reduced fertilization due to impaired sperm-egg fusion (17, 18).

As TM4SF proteins, CD81 and CD9 possess short cytoplasmic amino and carboxyl termini and a short cytoplasmic loop, all of which lack any obvious signaling motifs (19–21). Instead of signaling directly, TM4SF proteins may act as facilitators or adaptors (20) connecting a subset of cell-surface proteins to a network described as the tetraspan web (22). In this regard, CD81- and/or CD9-interacting proteins identified to date include Leu-13, CD19, CD21, HLA-DR, major histocompatibility complex I, CD4, CD8, $\alpha_3\beta_1$ integrin, $\alpha_4\beta_1$ integrin, $\alpha_6\beta_1$ integrin, other TM4SF members, CD37, CD53, CD63, CD82, and NAG-2 (5, 14, 22–30).

Associations between CD81 or CD9 and other molecules may be functionally meaningful. For example, antibodies to CD19 and CD81 both trigger homotypic aggregation (23), whereas a CD19 chimera that no longer associates with CD81 no longer mediates this effect (31). Also, B cells from CD81-null mice have reduced levels of cell-surface CD19 and impaired calcium fluxes in response to CD19 cross-linking (8–10). Other studies have shown that anti-CD81 antibodies may both stimulate (32) and interfere with (6, 33, 34) the functions of the CD81-associated integrins, and ectopic expression of CD9 may modulate integrin signaling (35).

Currently, little is known about the structural basis of the proposed TM4SF network. The large number of putative CD81- and CD9-associated proteins raises questions about the size of these complexes and the proximity and specificity of individual associations. In this regard, gel permeation analysis of TM4SF complexes in CHAPS lysates suggests that these complexes could be in excess of 20 × 10^6 Da (36). In addition, isopycnic sucrose gradient results suggest that many TM4SF associations may exist in the context of large detergent-resistant membrane microdomains (37, 38). Consistent with this, a large number of CD81 and CD9 associations are seen in relatively mild (*i.e.* permissive) detergents such as CHAPS, Tween 20, Brij 58, and Brij 99 (22, 39, 40) that are generally less able to disrupt microdomain-containing vesicles in cell lysates. The tendency of TM4SF proteins to associate with each other raises critical issues regarding specificity. For example, in CHAPS extracts of Raji cells, anti-CD37, anti-CD53, anti-CD82, and anti-CD81 antibodies all coprecipitated several major bands of identical molecular mass (27). When transfected into Raji cells, CD9 acquired a pattern of coprecipitating bands that was very

* This work was supported by National Institutes of Health Grant GM38903 (to M. E. H.). The costs of publication of this article were defrayed in part by the payment of page charges. This article must therefore be hereby marked "*advertisement*" in accordance with 18 U.S.C. Section 1734 solely to indicate this fact.

¶ To whom correspondence should be addressed: Dana-Farber Cancer Inst., Rm. D-1430, 44 Binney St., Boston, MA 02115. Tel.: 617-632-3410; Fax: 617-632-2662; E-mail: Martin_Hemler@dfci.harvard.edu.

[1] The abbreviations used are: TM4SF, transmembrane-4 superfamily; CHAPS, 3-[(3-cholamidopropyl)dimethylammonio]-1-propanesulfonate; mAb, monoclonal antibody; HRP, horseradish peroxidase; PAGE, polyacrylamide gel electrophoresis; HPLC, high pressure liquid chromatography; MβCD, methyl-β-cyclodextrin; FPRP, prostaglandin $F_2\alpha$ receptor regulatory protein.

similar to that of CD81 and CD82 (22). CD9 and CD63 immunoprecipitations from CHAPS extracts of MV3 and MEL-FC cells appeared very similar (41), and CD53, CD63, CD81, and CD82 precipitated from Brij 58 extracts of Molt-4 cells all yielded similar patterns of coprecipitating proteins, one of which was identified as $\alpha_4\beta_1$ integrin (30).

Resolution of TM4SF specificity and proximity issues may be facilitated by careful choice of detergent lysis conditions. Detergents such as CHAPS, Tween 20, Brij 58, and Brij 99 may be of limited utility because they yield perhaps too many TM4SF-associated proteins. On the other hand, a more stringent detergent such as Triton X-100 may be too disruptive with respect to TM4SF protein associations. A useful compromise may be a moderately stringent detergent such as Brij 96/97, which yields a restricted set of CD81 and CD9 associations. For example in 1% Brij 96, associations with $\alpha_3\beta_1$ and $\alpha_6\beta_1$ integrins are preserved, whereas other integrin associations (seen in CHAPS, Tween 20, Brij 58, and Brij 99) are lost (29, 42). Associations seen in Brij 96 have so far proven to be functionally relevant. For example, $\alpha_3\beta_1$·CD81 complexes contribute to neurite outgrowth (6), and CD81·CD19 complexes modulate B cell signaling (43).

Proteins so far shown to associate with CD81 or CD9 in Brij 96/97 conditions have not shown a very high stoichiometry. For example, in B cells, <10% of CD19 associated with CD81 and CD9 (44) and only 1–2% of CD4 associated with CD81 (45). Similarly, only a low level of $\alpha_3\beta_1$ integrin (10–20%) associated with CD81 or CD9 in various cell lines (29).[2] In addition, in Brij 96/97 conditions, major CD81-associated cell-surface proteins have been observed, but not yet characterized (*e.g.* see Refs. 29 and 44). Thus, our first goal here was to identify novel, prominent, CD81-associated protein(s) while using relatively stringent detergent conditions (Brij 96/97). Our second goal was to analyze novel CD81 complexes in terms of specificity, density, and estimated size. Our results point to complexes between CD81, CD9, and FPRP (the prostaglandin $F_{2\alpha}$ receptor regulatory protein) that are novel, robust, highly specific, and occur as discrete biochemical entities. The FPRP molecule is a type I integral membrane protein containing six extracellular immunoglobulin domains (46). It associates with the prostaglandin $F_{2\alpha}$ receptor and possibly other seven-transmembrane receptors and thereby reduces receptor ligand-binding capacity (47, 48). Aside from its associations with seven-transmembrane receptors, no other FPRP associations had been previously described.

MATERIALS AND METHODS

Antibodies—The anti-integrin mAbs used in this study were anti-α_2, A2-IIE10 (49); anti-α_3, A3-IIF5 (50); and anti-α_6, A6-BB.[2] The anti-TM4SF antibodies used were anti-CD9, DuALL (Sigma); anti-CD63, 6H1 (42); anti-CD81, M38 (51) and JS64 (52); anti-CD82, M104 (51); and anti-CD151, 5C11 (53) and TS151r (54). The anti-transferrin receptor mAbs used were OKT9 and HB21 (American Type Culture Collection). Rabbit polyclonal antisera specific for FPRP,[3] the α_{3A} integrin cytoplasmic domain (55), and caveolin (Transduction Laboratories) were also used. Horseradish peroxidase (HRP)-conjugated goat anti-mouse and goat anti-rabbit antibodies were from Transduction Laboratories.

Cell Culture—HT1080 fibrosarcoma cells, NT2 teratocarcinoma cells, and 293 cells were maintained in Dulbecco's modified Eagle's medium with 10% fetal bovine serum (Life Technologies, Inc.), penicillin/streptomycin, and 2 mM glutamine. Retinoic acid-treated NT2 cells (NT2RA cells) were obtained by treating NT2 cells with 10 μM retinoic acid for 4–5 weeks, splitting cells 1:6 into fresh flasks, and treating them for 10–14 days with mitotic inhibitors (56). These cells consist of a mixed population of neuron-like and non-neuronal cell types. NT2 neuron-like cells (NT2N cells) were purified from NT2RA cells as previously described (6). Purified neurons were maintained in serum-free Dulbecco's modified Eagle's medium with B27 supplements (Life Technologies, Inc.) (57) on plates coated with Matrigel (Becton Dickinson) diluted 1:30.

Immunoprecipitation and Immunoblotting—Cells were biotinylated with 0.2 mg/ml sulfosuccinimidyl 6-(biotinamido)hexanoate (Pierce) in 20 mM HEPES (pH 7.5), 150 mM NaCl, and 5 mM $MgCl_2$ (HBSM) for 1 h at room temperature. After three rinses with HBSM, cells were lysed by scraping into 1% Brij 96 (polyoxyethylene 10-oleyl ether; Fluka) in HBSM with 2 mM phenylmethylsulfonyl fluoride, 20 μg/ml aprotinin, and 10 μg/ml leupeptin. After a 1-h extraction at 4 °C with rocking, insoluble material was removed by centrifugation, and lysates were precleared for 1 h at 4 °C with protein G-Sepharose (Amersham Pharmacia Biotech). Specific antibodies were added along with protein G-Sepharose, and immune complexes were collected overnight at 4 °C. After rinsing four times with lysis buffer, immune complexes were eluted by boiling in sample buffer, resolved by SDS-PAGE, and transferred to nitrocellulose. Blots were blocked with 3% nonfat milk in phosphate-buffered saline with 0.1% Tween 20 (PBST). After rinsing with PBST, blots were developed with HRP-ExtrAvidin (Sigma) and diluted 1:3000 in PBST, followed by chemiluminescence. For immunoblotting, CD81-associated proteins were eluted from rinsed immune complexes with 1% Triton X-100 (Sigma) and 0.2% SDS in lysis buffer. Eluted proteins were separated by SDS-PAGE, transferred to nitrocellulose, and blocked with 5% nonfat milk in PBST or with 2% bovine serum albumin and 2% Tween 20 in phosphate-buffered saline (for FPRP blots). Blots were developed with diluted antibodies for α_3 integrin (1:1000), FPRP (1:300), caveolin (1:5000), or transferrin receptor (1:1 mixture of OKT9 and HB21 neat tissue culture supernatants), followed by HRP-conjugated goat anti-rabbit or goat anti-mouse antiserum (diluted 1:4000) and chemiluminescence.

Purification of CD81-associated Proteins—~7×10^8 NT2RA cells were lysed in a total of 12 ml of 1% Brij 96 lysis buffer and precleared as described above. Anti-CD81 antibody JS64 was added at 5 μg/ml along with 160 μl (settled volume) of protein G-Sepharose, and CD81 complexes were collected overnight at 4 °C. After extensive rinsing with lysis buffer, CD81-associated proteins were eluted by incubation with 1% Triton X-100 and 0.1% SDS in HBSM with 20 μg/ml aprotinin, 10 μg/ml leupeptin, and 2 mM phenylmethylsulfonyl fluoride for 10 min at 37 °C. Eluted proteins were collected in ~250 μl with a microcentrifuge filter unit (Costar Corp.). Using an Amido Black dye binding assay (58), we estimated that ~36 μg of CD81-associated proteins were recovered in the eluate. The eluate was concentrated with a Microcon-10 microconcentrator (Amicon, Inc.) and resolved by SDS-PAGE on an 11% minigel. CD81-associated proteins were revealed by silver staining, excised, rinsed with 50% HPLC-grade acetonitrile, and stored at −20 °C until analysis.

Nano Liquid Chromatography Ion Trap Tandem Mass Spectrometry and Sequencing—Silver-stained bands were subjected to in-gel reduction, carboxyamidomethylation, and tryptic digestion (Promega). Multiple peptide sequences were determined in a single run by microcapillary reverse-phase chromatography directly coupled to a Finnigan LCQ quadrupole ion trap mass spectrometer equipped with a custom nanoelectrospray source. The column was packed in-house with 5 cm of C_{18} support into a New Objective one-piece 75-μm inner diameter column terminating in an 8.5-μm tip. Flow rate was 190 nl/min. During chromatography, the ion trap repetitively surveyed full-scan mass spectra over the range of m/z 300–1400, executing data-dependent scans on the three most abundant ions in the survey scan. These scans allowed acquisition of a high resolution (zoom) scan to determine charge state and exact mass and tandem mass spectra for peptide sequence information. Tandem mass spectra were acquired with a relative collision energy of 30%, an isolation width of 2.5 Da, and recurring ions dynamically excluded. Interpretation of the resulting tandem mass spectra of the peptides was facilitated by programs developed in the Harvard Microchemistry Facility and by data base correlation with the algorithm Sequest (59, 60).

Sucrose Gradients—Brij 96 lysates of cell surface-biotinylated NT2RA cells were prepared as described above. Methyl-β-cyclodextrin (MβCD) in HBSM (final concentration of 10 mM) or an equivalent volume of HBSM alone was added to lysates containing ~2.4×10^7 cell equivalents, and lysates were incubated for 10 min at 25 °C. Lysates were then loaded in 45% sucrose (2 ml) over a 0.5-ml cushion of 50% sucrose and overlaid with layers of 40% sucrose (1 ml), 20% sucrose (1 ml), and 5% sucrose (0.5 ml) prepared in HBSM without detergent. Following centrifugation for 21 h at 45,000 rpm in a Beckman SW Ti-55 rotor at 4 °C, 14 fractions of 360 μl were collected from the tops of the gradients. The pellets were included in the final fraction of each gradi-

[2] C. S. Stipp and M. E. Hemler, unpublished data.
[3] D. Orlicky, unpublished data.

ent. 250 μl of each fraction were diluted with 750 μl of 1% Brij 96 in HBSM, and CD81 complexes were immunoprecipitated and analyzed as described above. Aliquots of each fraction were also analyzed by immunoblotting for FPRP, caveolin, and transferrin receptor.

Gel Permeation Chromatography—Cell surface-biotinylated 293 cells were lysed in 1% Brij 96 as described above. Lysate containing ~1×10^7 cell equivalents was loaded in 5% glycerol with blue dextran and phenol red onto a 25.5 × 1.0-cm Sepharose 6B column that had been pre-equilibrated in 1% Brij 96 in HBSM at room temperature (Brij 96 solutions cloud upon prolonged storage at 4 °C). 22 fractions of ~540 μl were collected, spanning from the leading edge of the blue dextran elution to the phenol red elution point. CD81 complexes were immunoprecipitated from each entire fraction and analyzed by SDS-PAGE as described above.

Immunodepletion—~4×10^7 293 cells were surface-biotinylated and lysed in 1% Brij 96 as described above. The lysate was divided into six equal portions to be immunodepleted four times with either protein G-Sepharose alone or with protein G-Sepharose plus mAb specific for CD9, CD81, CD151, α_3 integrin (all at 10 μg/ml), or α_6 integrin (1:20 dilution of ascites). The first three rounds of immunodepletion were for 60–90 min each; the final round was overnight at 4 °C. Triton X-100 (1% final concentration) was added, and each sample was further divided into six equal parts for immunoprecipitation with mAb specific for CD9, CD81, CD151, α_3 integrin, or α_6 integrin or with NeutrAvidin (Molecular Probes, Inc.) that had been coupled to Affi-Gel 10 (Bio-Rad). Samples were analyzed by SDS-PAGE and visualized with HRP-ExtrAvidin (antibody-precipitated samples) or by immunoblotting for FPRP (NeutrAvidin-precipitated samples).

RESULTS

CD81 and CD9 Complexes Are Distinct from Other TM4SF Complexes—To address the issue of TM4SF protein complex specificity, we first compared the profile of associated proteins for several TM4SF proteins in two different cell types. For these experiments, we lysed cells in 1% Brij 96 (same as Brij 97) because this detergent (*e.g.* in comparison with Brij 98/99, Brij 58, or CHAPS) often yields a narrower range of TM4SF-associated proteins. After cell-surface labeling with biotin, individual TM4SF complexes were immunoprecipitated from Brij 96 lysates. In retinoic acid-treated NT2 cells (NT2RA cells), the profiles of CD81- and CD9-associated proteins were virtually identical and were distinct from the profiles of other TM4SF proteins and integrins (Fig. 1*A*). For example, major CD9- and CD81-associated species migrating at ~40, 45, and 70 kDa (*asterisks*) were much less abundant in or completely absent from other TM4SF complexes. Conversely, a major 36-kDa species present in CD82 complexes was absent from CD9 and CD81 complexes. In 293 cells, CD81 and CD9 complexes were again virtually identical to each other and contained major species at ~52 and 70 kDa (Fig. 1*B*, *asterisks*) that were much less abundant in or absent from other TM4SF complexes. Common to all the TM4SF complexes was the presence of species above 120 kDa that comigrated with integrins. These results provide confidence that CD81 and CD9 complexes may be substantially distinct from other TM4SF complexes and from integrin complexes.

CD81 Complexes Contain a Major Unidentified 133-kDa Protein—To examine more carefully the integrin-like material in CD81 complexes, we prepared Brij 96 lysates and then fractionated CD81-associated proteins on low percentage SDS-polyacrylamide gels. In NT2RA cells, CD81 immunoprecipitation yielded coprecipitation of a major cell-surface biotin-labeled protein of ~133 kDa (Fig. 2*A*, *lane 1*). As seen by α_3 immunoblotting (*lane 2*), the ~133-kDa protein (*lane 1*) did not comigrate with the 150-kDa α_3 subunit of $\alpha_3\beta_1$ integrin, the major CD81-associated integrin on NT2 cells (6).

In a separate experiment, CD81 complexes from surface-biotinylated NT2RA cells were immunoprecipitated and dissociated with 1% Triton X-100 and 0.2% SDS, and then proteins were re-immunoprecipitated with mAb to α_3 (Fig. 2*B*, *lane 2*) or α_2 (*lane 3*). Again, the relatively small amount of *re-precipitated* $\alpha_3\beta_1$ (*lane 2*) appeared quite distinct from the 133-kDa protein *co-immunoprecipitated* with CD81 (*lane 1*). As expected, no $\alpha_2\beta_1$ integrin could be detected in association with CD81 in a Brij 96 lysate (*lane 3*). In contrast to NT2RA cells, HT1080 cells yielded CD81-coprecipitating material that resolved into bands consistent with α and β integrin subunits (Fig. 2*A*, *lane 3*). Immunoblotting of the α_3 integrin subunit (*lane 4*) confirmed that the upper band seen in *lane 3* indeed is the α_3 integrin subunit. In conclusion, NT2RA cells, but not HT1080 cells, possess a major CD81-associated protein of ~133 kDa that is not an integrin.

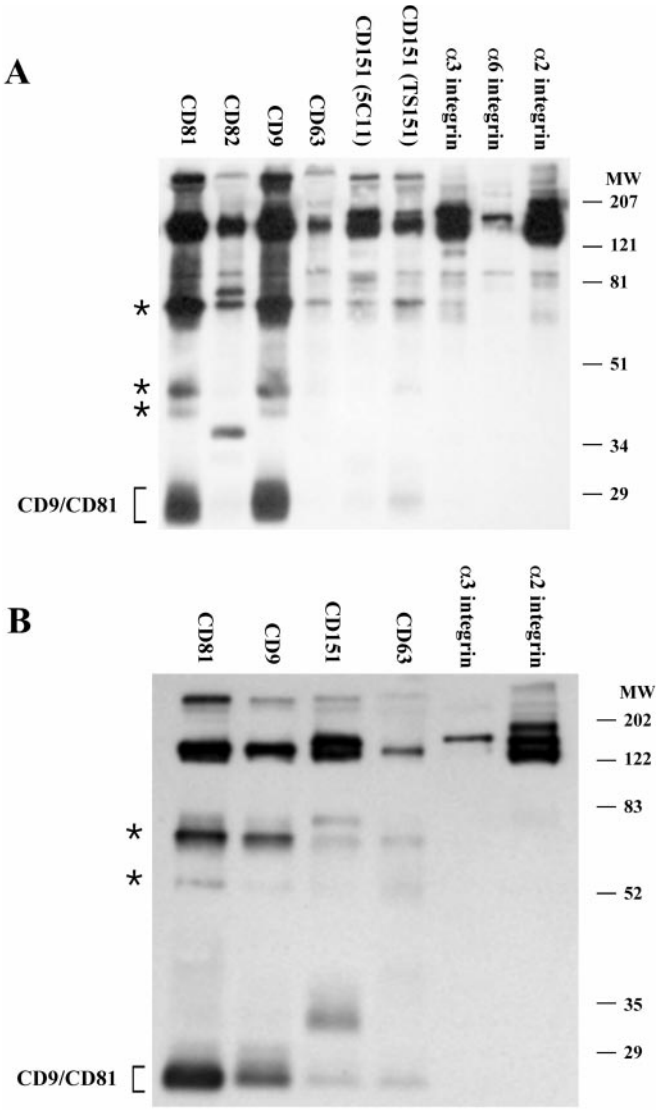

FIG. 1. **CD81 and CD9 complexes are distinct from other TM4SF complexes.** *A*, ~3×10^7 NT2RA cells were cell surface-labeled with biotin and lysed in 5.5 ml of 1% Brij 96. Equal portions of the lysate were immunoprecipitated with antibodies to the indicated TM4SF proteins and integrins. Complexes were resolved by SDS-PAGE on an 11% acrylamide gel, transferred to nitrocellulose, and visualized by HRP-ExtrAvidin, followed by chemiluminescence. Two different anti-CD151 antibodies were used (5C11 and TS151r). *Asterisks* indicate bands unique to or highly enriched in CD9 and CD81 complexes. *B*, ~2×10^7 293 cells were labeled with biotin and analyzed as described for *A*.

Identification of FPRP as a Major CD81-associated Protein—To identify the 133-kDa species, we prepared CD81 immune complexes from Brij 96 lysates of NT2RA cells, and CD81-associated proteins were eluted with 1% Triton and 0.2% SDS (see "Materials and Methods"). SDS-PAGE analysis of 6 μg of CD81-associated proteins, followed by silver staining,

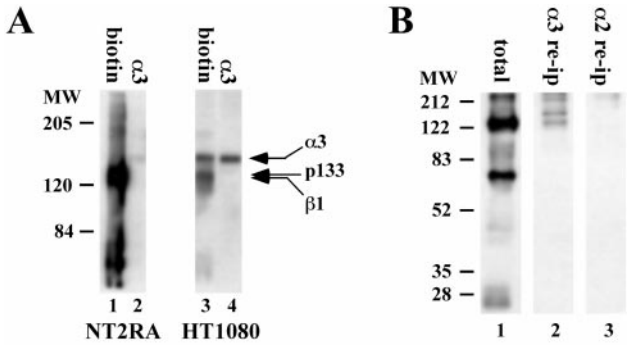

FIG. 2. **An unidentified 133-kDa protein in CD81 complexes from NT2RA cells.** *A*, NT2RA and HT1080 cells were cell surface-biotinylated and lysed in 1% Brij 96. CD81 complexes were immunoprecipitated, eluted in 1% Triton X-100 and 0.2% SDS, and separated by SDS-PAGE on a 7% acrylamide gel. To detect all CD81-associated biotin-labeled proteins, blotting was carried out using HRP-ExtrAvidin (*lanes 1* and *3*). Alternatively, an anti-α_3 integrin polyclonal antibody was used for blotting (*lanes 2* and *4*). The locations of α_3 and β_1 integrin subunits and an unidentified 133-kDa protein are indicated. *B*, CD81 complexes were immunoprecipitated from a Brij 96 lysate from ~8×10^7 biotin-labeled NT2RA cells. CD81-associated proteins were eluted from the complexes in 1% Triton X-100 and 0.2% SDS. Next, 11% of the eluate was analyzed directly (*lane 1*), and 33% was re-immunoprecipitated (*re-ip*) with an anti-α_3 integrin mAb (*lane 2*) or an anti-α_2 integrin mAb (*lane 3*). Proteins were visualized by blotting with HRP-ExtrAvidin after SDS-PAGE.

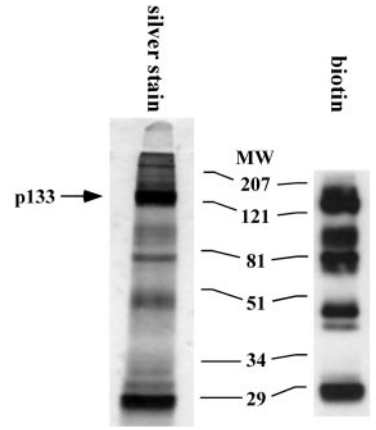

FIG. 3. **Comparison of silver-stained and cell surface-biotinylated CD81 complexes.** ~6 μg of CD81-associated proteins prepared from ~1×10^8 NT2RA cells were fractionated by SDS-PAGE and visualized by silver staining. For comparison, cell surface-biotinylated CD81-associated proteins prepared from ~1.5×10^7 NT2RA cells were analyzed by blotting with HRP-ExtrAvidin. The location of the major 133-kDa CD81-associated protein is indicated.

again revealed a major 133-kDa species that was apparently more abundant than any other CD81-associated protein (Fig. 3, *left lane*). Next, ~36 μg of CD81-associated proteins were fractionated by SDS-PAGE, and silver-stained material above 120 kDa was excised for further analysis. Proteins were digested *in situ* with trypsin, and the eluted tryptic peptides were separated by reverse-phase liquid chromatography and sequenced by ion trap tandem mass spectrometry. We obtained sequence information for one peptide derived from the β_1 integrin subunit and eight peptides derived from FPRP, a cell-surface Ig superfamily protein (46) (Table I). The reported molecular mass of FPRP (133–135 kDa) is fully consistent with our protein identification.

To verify that FPRP associates with CD81, we analyzed CD81 immunoprecipitates by immunoblotting with an anti-FPRP polyclonal antibody. The anti-FPRP polyclonal antibody recognized a single band from NT2RA cells (Fig. 4, *lane 3*) and from 293 cells (*lane 9*) that precisely comigrated with the major 133-kDa band seen in total cell surface-biotinylated CD81-associated proteins (*lanes 1* and *7*). The α_3 integrin was present at a much lower level in CD81 complexes from NT2RA and 293 cells and migrated above FPRP (*lanes 2* and *8*), in agreement with Fig. 2. Again in agreement with Fig. 2, CD81 complexes from HT1080 cells contained minimal FPRP (*lane 6*), whereas $\alpha_3\beta_1$ integrin was abundant (*lanes 4* and *5*). In conclusion, the major 133-kDa CD81-associated protein detected by cell-surface biotinylation in two out of three cell lines is confirmed to be FPRP.

FPRP Associates Specifically with CD81 and CD9—To determine whether FPRP associates with other TM4SF proteins and/or integrins, TM4SF and integrin immunoprecipitates were prepared from Brij 96 lysates and then blotted for FPRP. FPRP was detected specifically in CD81 complexes, but not in CD151, α_2, or α_3 complexes from 293, NT2N, and HT1080 cells (Fig. 5, *A–C*). FPRP was also not present in CD63 complexes (from 293 and HT1080 cells) and was not seen in α_6 complexes from NT2N cells. Results showing FPRP present in CD81 immunoprecipitates from HT1080 cells (Fig. 5*C*) do not contradict results in Fig. 4 (*lane 6*) because a much longer immunoblot exposure time was used in Fig. 5*C*.

TABLE I
Peptide sequences of CD81-associated proteins

FPRP[a]	β_1 integrin subunit
TANDAVELHIK	LSENNIQTIFAVTEEFQPVYK
APVLLSSLDRK	
VDGVVLEK	
MDVLNAFK	
YIISLDQDSVVK	
TTEEDRGNYYCVVSAWAR	
SYHLLVR	
MYQTQVSDAGLYR	

[a] These peptide sequences, derived from the human protein, exactly match the sequence of murine FPRP. The full-sequence of human FPRP is not yet available.

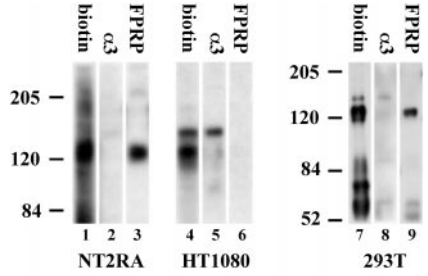

FIG. 4. **FPRP is a major CD81-associated protein.** NT2RA cells (*lanes 1–3*), HT1080 cells (*lanes 4–6*), and 293 cells (*lanes 7–9*) were cell surface-biotinylated and lysed in 1% Brij 96. CD81 complexes were immunoprecipitated, and CD81-associated proteins were eluted in 1% Triton X-100 and 0.2% SDS and separated by SDS-PAGE. Eluate equivalent to ~2.5×10^6 cells was analyzed by blotting with HRP-ExtrAvidin (*lanes 1*, *4*, and *7*), anti-α_3 integrin polyclonal antibody (*lanes 2*, *5*, and *8*), or anti-FPRP polyclonal antibody (*lanes 3*, *6*, and *9*).

Because CD9 and CD81 yielded virtually identical patterns of coprecipitating proteins in multiple cell lysates (see Fig. 1 above), it was not unexpected that CD9 immunoprecipitates from 293 cells would also contain FPRP (Fig. 5*A*). It is unlikely that CD9 is required for CD81-FPRP association since CD81·FPRP complexes were observed in two cell lines (NT2N and HT1080) (Fig. 5, *B* and *C*) that lack CD9 (6, 29).

CD81-FPRP Association Is Not Lipid Raft-dependent—Lipid rafts are membrane microdomains, stabilized by a high content of cholesterol, sphingolipids, and phospholipids with long, saturated fatty acyl side chains (61, 62). The importance of cholesterol is underscored by the raft-destabilizing effect of the cholesterol-depleting agent MβCD (63). Many raft-localized

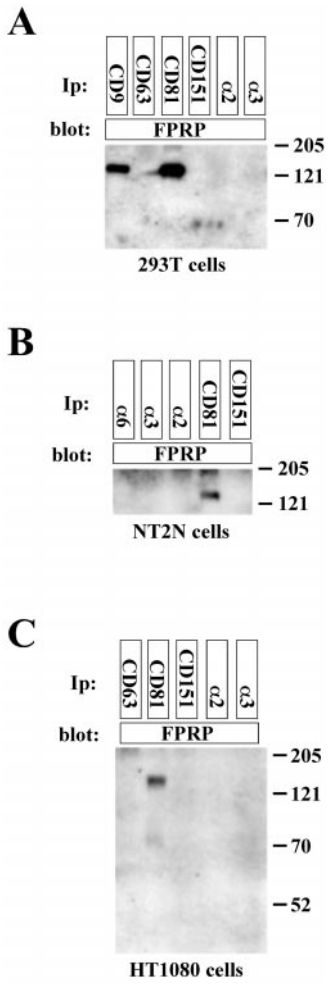

FIG. 5. **FPRP associates specifically with CD81 and CD9.** *A*, a Brij 96 lysate prepared from 293 cells was immunoprecipitated (*Ip*) with mAbs against the indicated TM4SF proteins and integrin subunits. Immunoprecipitates were eluted with 1% Triton X-100 and 0.2% SDS, and eluates equivalent to $\sim 3 \times 10^6$ cells were analyzed by immunoblotting for FPRP. Independent experiments confirmed that antibodies used for immunoprecipitation could recognize abundant CD9, CD63, CD151, α_2, and α_3 from 293 cells (*e.g.* see Fig. 7 and not shown). *B*, a Brij 96 lysate of NT2N cells was analyzed as described for *A* ($\sim 2 \times 10^6$ cell equivalents/lane). *C*, a Brij 96 lysate of HT1080 cells was analyzed as described for *A* ($\sim 3 \times 10^6$ cell equivalents/lane). The antibodies utilized each immunoprecipitated their respective antigens from NT2N and HT1080 cells, as seen in Fig. 1.

molecules are resistant to extraction with cold nonionic detergents, and the high ratio of lipid to protein causes the segregation of rafts into the low density fractions (containing between 5 and 25% sucrose) of isopycnic sucrose gradients. Because TM4SF proteins (38, 64) and integrins (65–67) may sometimes localize into lipid raft-like domains (61, 62), we considered that CD81·CD9·FPRP complexes may occur in, or perhaps even depend on, raft-like domains.

Here we analyzed CD81·CD9·FPRP complexes to determine (i) whether they would localize to low density "light membrane" fractions of sucrose gradients, and (ii) if they would be perturbed upon cholesterol depletion with MβCD. Untreated Brij 96 lysate was fractionated on a sucrose gradient, and CD81 complexes were then immunoprecipitated from each fraction. As shown in Fig. 6*A* (*upper panel*), CD81, CD9, and the 133-kDa FPRP protein were broadly distributed, with the majority of the material in fractions 4–10 (20–45% sucrose) and a small percentage of each protein in fractions 1–3 at the top of the gradient. Upon addition of MβCD to the lysate prior to centrifugation, CD81, CD9, and the 133-kDa FPRP protein were depleted from the upper fractions of the gradient, but the complexes remained intact in the denser fractions (*lower panel*). Immunoblotting of CD81 immunoprecipitates with anti-FPRP polyclonal antibody confirmed that FPRP remained associated with CD81 in either the presence or absence of MβCD (Fig. 6*B*, *upper* and *lower panels*). Unfortunately, the limited sensitivity of the anti-FPRP polyclonal antibody precluded detection of FPRP weakly present in fractions 1–3. Nonetheless, a shift in CD81-associated FPRP toward the denser fractions such as seen in Fig. 6*A* was confirmed in Fig. 6*B*.

The identity of other CD81-associated proteins (*e.g.* the ~75-kDa protein seen in Fig. 6*A*) remains to be determined. Notably, a 45-kDa protein species (Fig. 6*A*, *upper panel*, *open arrow*) was no longer detected after MβCD treatment (*lower panel*), suggesting that at least one protein may indeed require cholesterol for CD81 association. Caveolin, a positive control marker of cholesterol-enriched light membranes, localized primarily to the top four sucrose gradient fractions (Fig. 6*C*, *upper panel*). As expected, MβCD treatment substantially shifted caveolin away from the low density fractions, such that most moved to the bottom of the gradient (fraction 14), whereas some remained in fractions 3–5 (*lower panel*). This caveolin was largely non-overlapping with CD81, CD9, and FPRP. The transferrin receptor, a non-raft marker, localized somewhat below the majority of the CD81 complexes in the sucrose gradient (predominantly in fractions 6–12) and was largely unaffected by MβCD treatment (Fig. 6*D*).

For an even more rigorous test of cholesterol dependence of the CD81·CD9·FPRP complex, we incubated cell surface-biotinylated, immunopurified CD81 complexes with increasing concentrations of MβCD prior to analysis by SDS-PAGE. As shown in Fig. 6*E* (*upper panel*), even 100 mM MβCD failed to disrupt the complex. Only the 45-kDa species noted in Fig. 6*A* was eliminated by MβCD treatment (*open arrow*). Immunoblotting of an aliquot of each sample for FPRP confirmed that MβCD had no effect on the amount of FPRP associated with CD81 (*lower panel*). In conclusion, the CD81·CD9·FPRP complex may partially associate with a raft-like microdomain distinct from caveolin-containing microdomains, but CD81-CD9-FPRP association is not dependent on raft localization.

Stoichiometry of CD81-CD9-FPRP Association—To estimate the fraction of FPRP that is associated with CD81 and CD9, we performed immunodepletion experiments. Brij 96 lysates of surface-biotinylated 293 cells were subjected to four rounds of immunodepletion using either no antibody or anti-CD9, anti-CD81, anti-CD151, anti-α_3 integrin, or anti-α_6 integrin mAb. Triton X-100 was then added to each sample to dissociate complexes, and the remaining amount of FPRP, CD9, CD81, CD151, α_3 integrin, and α_6 integrin in each depleted sample was determined. As shown in Fig. 7 (*upper panel*), immunodepletion of either CD9 or CD81 removed essentially all detectable FPRP. Control depletion experiments (*second* and *third panels*) confirmed that the immunodepletion protocol had removed nearly all CD9 and CD81, respectively. Interestingly, CD81 immunodepletion removed much of the CD9 in the lysate, but CD9 immunodepletion had a minimal effect on the level of CD81. Thus, most CD9 must be associated with CD81, whereas CD81 is in substantial excess of CD9.

Immunodepletion of CD151, α_3 integrin, or α_6 integrin removed little if any surface-labeled FPRP from the 293 cell lysate. In contrast, CD151 immunodepletion removed a significant amount of the α_3 integrin, consistent with the high stoichiometry of the α_3·CD151 complex observed previously (53). CD151 immunodepletion also removed as much α_6 integrin as α_6 immunodepletion itself, indicating that the α_6·CD151 complex is also highly stoichiometric in 293 cells. Together, these

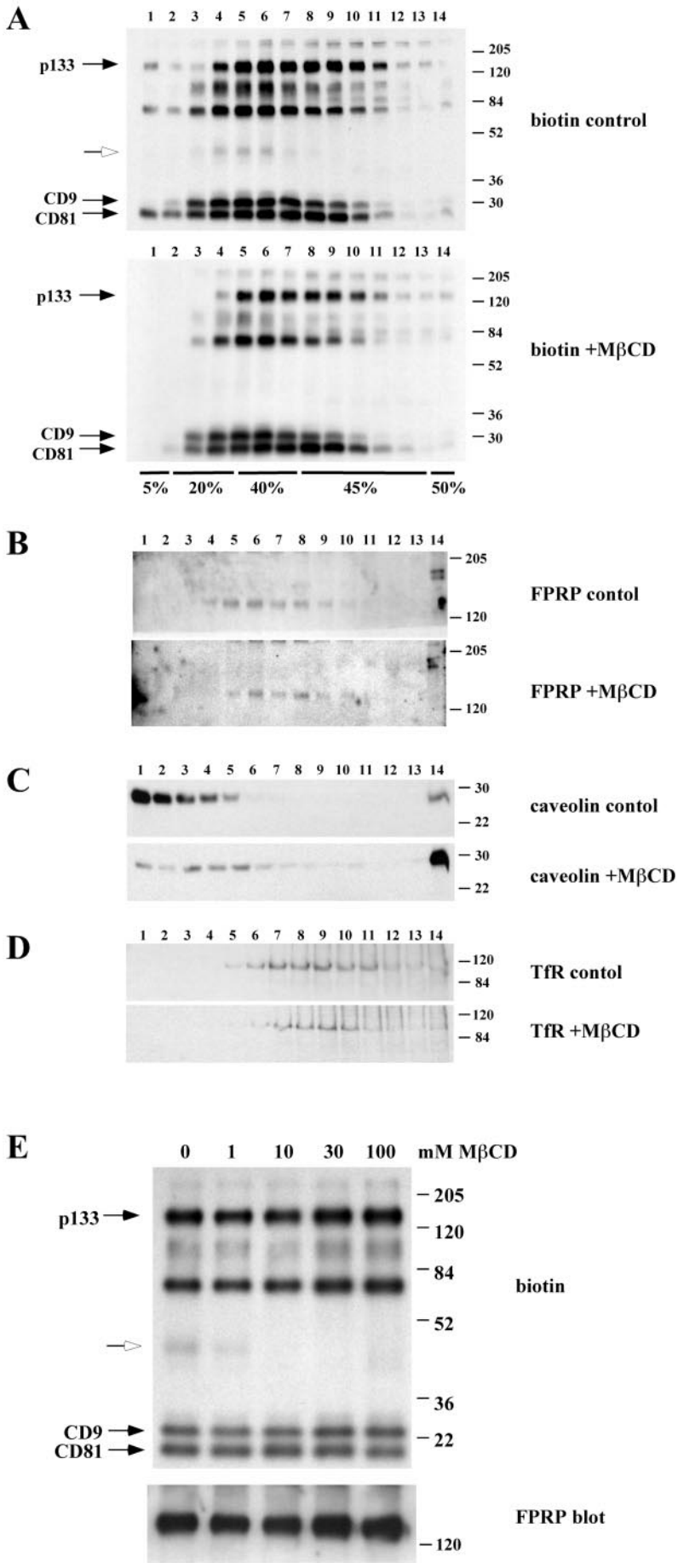

FIG. 6. **Effect of MβCD on CD81 complexes.** *A*, a Brij 96 lysate was prepared from ~4.8×10^7 cell surface-biotinylated NT2RA cells. The lysate was divided in half and left untreated (*control*) or treated with 10 mM MβCD for 10 min at room temperature (*MβCD*). Lysates were loaded in 2 ml of 45% sucrose over a 0.5-ml 50% sucrose cushion and overlaid with 40% (1 ml), 20% (1 ml), and 5% sucrose (0.5 ml) prepared without detergent. After centrifugation to equilibrium, 14 fractions of 360 μl were collected from the top of the gradient; the pellet was included in the final fraction. 250 μl of each fraction were used for immunoprecipitation with an anti-CD81 mAb, and CD81 complexes were analyzed by SDS-PAGE and blotting with HRP-ExtrAvidin. The locations of CD9, CD81, and the major 133-kDa CD81-associated protein are indicated by *closed arrows*. The *open arrow* indicates an unknown 45-kDa species. *B*, a Brij 96 lysate prepared from ~4.8×10^7 unlabeled NT2RA cells was treated and fractionated on sucrose gradients as described for *A*. CD81 complexes were immunoprecipitated from 250 μl of each fraction, and CD81-associated proteins were eluted from the complexes with 1% Triton X-100 and 0.2% SDS and then analyzed by immunoblotting for FPRP. *C*, 20 μl of each fraction from the gradients in *B* were analyzed by immunoblotting for caveolin. *D*, 20 μl of each fraction from the gradients in *B* were analyzed by immunoblotting for the transferrin receptor (*TfR*). All gradients in *A–D* were centrifuged simultaneously. *E*, ~3×10^7 cell surface-biotinylated NT2RA cells were lysed in 1% Brij 96, and CD81 complexes were immunoprecipitated. CD81 complexes bound to protein G-Sepharose were divided into equal portions and extracted with the indicated concentrations of MβCD for 15 min at 37 °C. Complexes remaining after extraction were eluted by boiling in SDS-PAGE sample buffer, and 20% of each sample was analyzed by blotting with HRP-ExtrAvidin (*upper panel*). The remaining 80% was analyzed by immunoblotting for FPRP (*lower panel*). The locations of CD9, CD81, and p133 are indicated by *closed arrows*, and the location of a 45-kDa band removed by MβCD treatment is indicated by the *open arrow*.

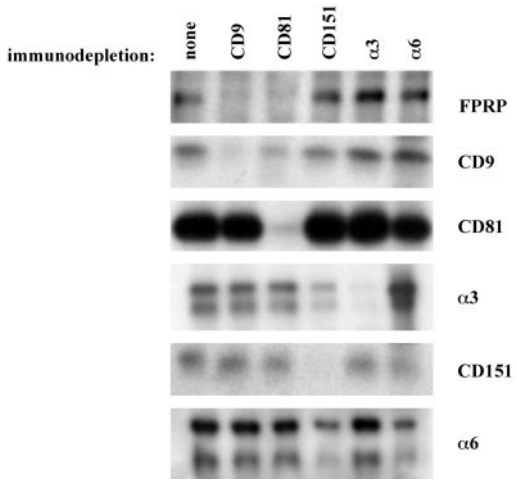

FIG. 7. **Highly stoichiometric association of FPRP with CD81 and CD9.** ~4 × 10^7 293 cells were surface-labeled with biotin and extracted with 1% Brij 96. The extract was divided into equal portions and depleted with protein G-Sepharose alone or with protein G plus mAb specific for CD9, CD81, CD151, α_3 integrin, or α_6 integrin. After four rounds of immunodepletion, Triton X-100 was added to 1%, and each portion was further divided into six aliquots. One aliquot was precipitated with NeutrAvidin-agarose, followed by blotting with an anti-FPRP polyclonal antibody. (Note that our anti-FPRP polyclonal antibody was not suitable for immunoprecipitations.) The remaining aliquots were immunoprecipitated with mAb specific for CD9, CD81, α_3 integrin, CD151, or α_6 integrin, followed by blotting with HRP-ExtrAvidin.

results suggest that specific TM4SF protein complexes (*e.g.* CD81·CD9·FPRP, α_3·CD151, and α_6·CD151) each occur at high stoichiometry (at least with respect to CD9, FPRP, α_3, and α_6), but fail to interact substantially with each other in Brij 96 lysates.

Different CD81 Complexes Have Distinct Sizes—For further analysis of CD81 complexes, we utilized gel permeation chromatography. A cell surface-biotinylated Brij 96 extract of 293 cells was fractionated on a Sepharose 6B column, and then CD81 complexes were immunoprecipitated from each fraction and analyzed by SDS-PAGE. All of the CD81 complexes eluted significantly before the approximate void volume of the column as measured by the leading edge of dextran blue (shown in Fig. 8*A*; quantified in Fig. 8*B*). Thus, in Brij 96 lysates, CD81 complexes exist as discrete units of limited size (<4 × 10^6 Da). The 133-kDa FPRP protein eluted in a broad peak centered in fractions 6–10. These peak fractions also contained comparatively small amounts of labeled CD9 and CD81. (Note that surface labeling of TM4SF proteins may be blocked by TM4SF-associated molecules.) These results indicate that most CD81·FPRP complexes also contain CD9 in 293 cells.

Whereas CD81-associated FPRP peaked in fractions 7 and 8, the bulk of labeled CD81 peaked in fractions 11–16 (Fig. 8). Thus, we roughly estimate that 30–50% of labeled CD81 may not be associated with FPRP. In addition, an unknown CD81-associated 75-kDa protein (p75) peaked in fractions 8–10, suggesting that this complex is at least partly distinct from the CD81·FPRP complex. Also, levels of CD9 appearing in fractions 10–13 suggest that some p75·CD9·CD81 and/or CD81·CD9 complexes are present and are distinct from CD81·FPRP complexes.

DISCUSSION

Identification of a Novel CD81 (and CD9)-associated Protein—Our primary goal was to identify novel components abundantly present in CD81 protein complexes. However, it was first necessary to address the issue of TM4SF specificity, given the tendency of TM4SF proteins to associate with each other and with so many other proteins. In this regard, we established that CD81 and CD9 complexes can have a composition that is quite distinct from that of other TM4SF complexes (CD82, CD63, and CD151) and integrin complexes (α_3, α_6, and α_2). A key to these experiments was the use of 1% Brij 96/97 detergent. Less stringent detergents such as CHAPS, Brij 58, and Brij 98/99 tend to yield more extensive TM4SF protein complexes, in which the components associated with several distinct TM4SF proteins appear to be identical. In contrast, the more hydrophobic nature of Brij 96/97 yields a more restrictive pattern of TM4SF-associated proteins (see the Introduction).

Analysis of immunopurified CD81 complexes by cell-surface biotin labeling or by silver staining revealed that in some cell lines, one of the most prominent CD81-associated proteins was a potentially novel protein of 133 kDa, distinct from integrins. By ion trap tandem mass sequencing, this 133-kDa protein was identified definitively as FPRP. FPRP is an Ig superfamily protein with six Ig domains that was originally copurified with a prostaglandin $F_{2\alpha}$-binding fraction (46, 68). FPRP possesses no prostaglandin $F_{2\alpha}$-binding activity of its own and, in fact, down-regulates prostaglandin $F_{2\alpha}$ binding to COS cells when cotransfected with the prostaglandin $F_{2\alpha}$ receptor (47).

The CD81·FPRP complex was elevated in some cell lines (293 kidney epithelial cells and NT2RA neuronal cells) and less abundant in others (HT1080 fibrosarcoma cells). When FPRP was present at high levels (*e.g.* in 293 cells), not only was it one of the most abundant CD81-associated proteins, but it also showed very high stoichiometry, with nearly 100% of surface-labeled FPRP associating with both CD81 and CD9. In contrast, previously reported CD81- and CD9-associated proteins such as $\alpha_3\beta_1$ integrin, CD19, and CD4 showed a much lower stoichiometry (*i.e.* 1–20%; see the Introduction). In previous cases in which high stoichiometry interactions of various proteins with CD9 or CD81 have been observed, these were seen using less stringent detergents such as CHAPS, Brij 99, and Brij 35 (22, 64, 69). The only other TM4SF complexes so far reported to approach 80–100% stoichiometry in relatively restrictive detergent conditions are the $\alpha_3\beta_1$·CD151 and $\alpha_6\beta_1$·CD151 complexes (Refs. 53 and 54; see also Fig. 7).

Specificity, Size, and Density of TM4SF Protein Complexes—Our secondary goal was to examine issues of TM4SF complex specificity, size, and density. Our observations confirm that under appropriate detergent conditions, CD81 and CD9 complexes contain unique components not found in other TM4SF complexes. Indeed, we detected FPRP specifically in CD81 and CD9 complexes and not in CD63, CD151, α_2 integrin, α_3 integrin, and α_6 integrin complexes. Although both FPRP and α_3 integrin associated with CD81 in 293 cells, FPRP was not detected in α_3 immunoprecipitates, and α_3 immunodepletion removed no FPRP from 293 cell lysates. Furthermore, $\alpha_3\beta_1$ association with CD81 and CD9 could be readily observed in HT1080 cells (29), which have only low levels of FPRP; and conversely, CD81·CD9·FPRP complexes were abundant in 293 lysates, which have relatively low levels of $\alpha_3\beta_1$. When 293 cells were made to overexpress $\alpha_3\beta_1$ integrin, the amount of FPRP associated with CD81 was not decreased.[2] Thus, $\alpha_3\beta_1$·CD81 (or $\alpha_3\beta_1$·CD9) complexes are distinct from CD81·CD9·FPRP complexes.

Sucrose density gradients and gel filtration experiments revealed further differences among CD81 complexes. For example, complexes containing major unidentified 75- and 90-kDa species were less dense and a little smaller than CD81 complexes containing p133/FPRP. A CD81 complex with an unknown 45-kDa protein was also seen in the lower density sucrose fractions, and this complex, unlike any of the others, was uniquely dependent on cholesterol. Gel permeation chro-

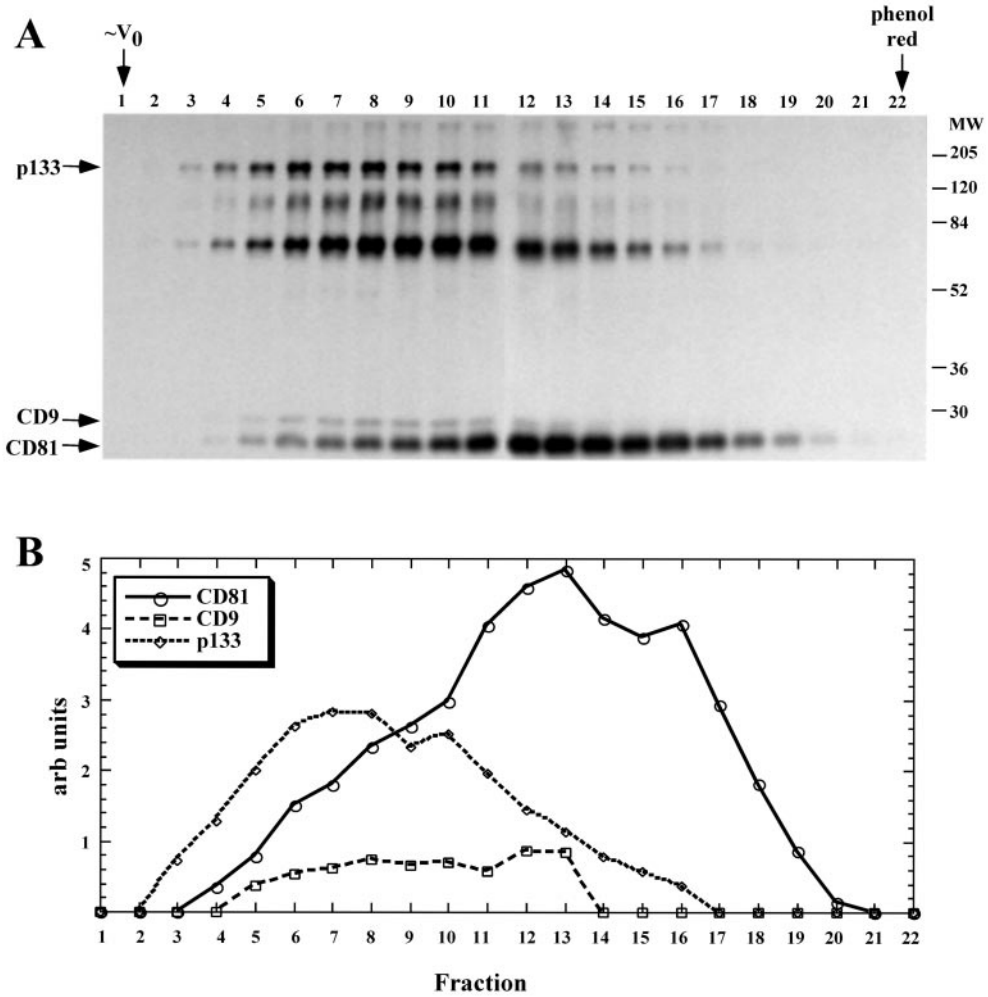

FIG. 8. **Gel permeation analysis of CD81 complexes.** *A*, a Brij 96 lysate from ~1×10^7 surface-biotinylated 293 cells was fractionated on a Sepharose 6B column (25.0 × 1.0 cm) equilibrated in 1% Brij 96. 22 fractions of ~540 μl were collected from the leading edge of blue dextran (approximating V_0) to phenol red (indicating the small molecule elution point). CD81 complexes were immunoprecipitated from each fraction and analyzed by SDS-PAGE, followed by blotting with HRP-ExtrAvidin. The locations of CD9, CD81, and p133/FPRP are indicated. *B*, the elution profile in *A* was quantified by densitometry using the program Scion Image Version 1.62. The densities of CD9, CD81, and p133, expressed in arbitrary (*arb*) units, are plotted *versus* fraction number.

matography also revealed that a substantial pool of CD81 may exist in an uncomplexed state on the surface of 293 cells. These results provide evidence that TM4SF protein complexes may exist as discrete units, rather than as large vesicular aggregates.

The physical basis for the CD81-CD9-FPRP association is unclear. Because essentially all FPRP was associated with CD9, as well as with CD81, and nearly all CD9 was associated with CD81, one must conclude that essentially all FPRP was present in a CD81·CD9·FPRP complex on 293 cells. However, on HT1080 cells, CD81 associated with FPRP in the absence of CD9, indicating that CD9 is not necessary for complex formation. It remains to be determined whether CD9 would associate with FPRP in the absence of CD81. Because CD9 and CD81 share more sequence similarity with each other than with most other TM4SF proteins, one may hypothesize that these two TM4SF proteins may share an FPRP association site.

In preliminary experiments, we found no evidence for CD81 being directly cross-linked to FPRP.[2] However, this does not rule out a direct protein-protein interaction. The CD81 and FPRP molecules simply may lack appropriate functional groups in proximity to the interaction site. As an alternative, we considered the possibility that CD81, CD9, and FPRP associate via their mutual localization to detergent-insoluble, cholesterol-enriched membrane microdomain rafts. Although a small fraction of CD81·CD9·FPRP complexes could indeed colocalize with caveolin in low density fractions of isopycnic sucrose gradients, the majority of CD81·CD9·FPRP complexes resided in denser fractions. Furthermore, MβCD disruption of cholesterol-dependent microdomains failed to dissociate CD81·CD9·FPRP complexes, even though it was sufficient to displace caveolin and a subset of CD81·CD9·FPRP complexes from low density fractions. In fact, all CD81-associated proteins remained present, with the exception of a weakly biotinylated 45-kDa species (mentioned above). As seen here for CD81·CD9·FPRP complexes, we have found elsewhere that $\alpha_3\beta_1$·CD9 and $\alpha_3\beta_1$·CD81 complexes may localize to cholesterol-rich raft-type microdomains, but appear not to require cholesterol or raft localization to remain intact (64).

The majority of the CD81 complexes in sucrose gradients were clearly more dense than typical light membrane complexes (such as those containing caveolin) found at the 5–20% sucrose interface. However, even after cholesterol depletion, CD81 complexes did appear to be somewhat more buoyant than the transferrin receptor, a marker for typical well solubilized proteins. The basis of this slight increase in buoyancy is unclear, but one possibility is that TM4SF complexes may contain lipids other than cholesterol such as sphingolipids and long chain unsaturated phospholipids. Also, TM4SF proteins may display increased buoyancy due to acylation (70, 71).

Possible Functional Relevance—The mechanism whereby FPRP negatively regulates prostaglandin $F_{2\alpha}$ binding is unclear, but deletion mutagenesis suggested that this activity may map largely to the transmembrane and cytoplasmic regions of FPRP (47). The membrane-proximal Ig domain of FPRP contains a hydrophobic face that is proposed to interact with the membrane or another protein. It is not yet clear whether this hydrophobic face might interact with CD81 or CD9. The cytoplasmic domain of FPRP contains a potential protein kinase C phosphorylation site as well as a potential calmodulin-dependent protein kinase phosphorylation site. These are of potential relevance to CD81-mediated signaling events because of the association of protein kinase C with TM4SF complexes[4] and the ability of anti-CD81 antibodies to trigger calcium fluxes under certain conditions (23). In addition to the prostaglandin $F_{2\alpha}$ receptor, FPRP may regulate the function of other G protein-coupled receptors, including the β-adrenergic receptor (48), suggesting that FPRP may associate with a range of seven-transmembrane G protein-coupled receptors. It will be of interest to determine whether G protein-coupled receptors can also be detected in CD81 or CD9 complexes.

A portion of CD81·CD9·FPRP complexes appear in the light membrane fractions of sucrose gradients, and this localization is lost upon cholesterol depletion (*e.g.* see Fig. 6*A*). Thus, we propose that CD81·CD9·FPRP complexes may associate with lipid rafts. Indeed, studies elsewhere have also suggested that CD9 and CD81 may associate with lipid rafts (38, 64). In this manner, CD81·CD9·FPRP complexes perhaps could be brought into proximity with raft-associated signaling events, involving G proteins, Src family kinases, and phosphoinositide metabolism.

Oocyte CD9 clearly plays a major role during fertilization (17, 18). However, it is not yet clear whether FPRP is also present on oocytes. If present, it would be of obvious interest to consider a potential role for CD9·FPRP complexes during fertilization. The binding of hepatitis C virus to CD81 is of likely relevance to liver dysfunction and altered B lymphocyte proliferation (7). However, by Northern blotting, FPRP appears to be absent from liver and spleen (46), so it appears unlikely that FPRP would play a role during hepatitis C virus binding to CD81.

In conclusion, we have identified FPRP as a major component of CD81 and CD9 complexes in certain cell types. FPRP associates with CD81 and CD9 with high specificity and unprecedented stoichiometry. The limited size, high density, and specificity of CD81·CD9·FPRP complexes indicate that these exist as discrete biochemical entities, distinct from other TM4SF complexes. The association of a portion of CD81·CD9·FPRP complexes with lipid raft-type microdomains suggests a proximity to major signaling pathways. Together, these studies establish a novel link between TM4SF proteins and the FPRP molecule and thus provide important new insights into the activities of CD81, CD9, and FPRP.

Acknowledgments—We gratefully acknowledge W. S. Lane, R. Robinson, and K. Pierce (Harvard Microchemistry Facility) for expertise in HPLC, mass spectrometry, and peptide sequencing.

REFERENCES

1. Oren, R., Takahashi, S., Doss, C., Levy, R., and Levy, S. (1990) *Mol. Cell. Biol.* **10,** 4007–4015
2. Fearon, D. T., and Carter, R. H. (1995) *Annu. Rev. Immunol.* **13,** 127–149
3. Boismenu, R., Rhein, M., Fischer, W. H., and Havran, W. L. (1996) *Science* **271,** 198–200
4. Witherden, D. A., Boismenu, R., and Havran, W. L. (2000) *J. Immunol.* **165,** 1902–1909
5. Tachibana, I., Bodorova, J., Berditchevski, F., Zutter, M. M., and Hemler, M. E. (1997) *J. Biol. Chem.* **272,** 29181–29189
6. Stipp, C. S., and Hemler, M. E. (2000) *J. Cell Sci.* **113,** 1871–1882
7. Pileri, P., Uematsu, Y., Campagnoli, S., Galli, G., Falugi, F., Petracca, R., Weiner, A. J., Houghton, M., Rosa, D., Grandi, G., and Abrignani, S. (1998) *Science* **282,** 938–941
8. Maecker, H. T., and Levy, S. (1997) *J. Exp. Med.* **185,** 1505–1510
9. Tsitsikov, E. N., Gutierrez-Ramos, J. C., and Geha, R. S. (1997) *Proc. Natl. Acad. Sci. U. S. A.* **94,** 10844–10849
10. Miyazaki, T., Muller, U., and Campbell, K. S. (1997) *EMBO J.* **16,** 4217–4225
11. Kersey, J. H., LeBien, T. W., Abramson, C. S., Newman, R., Sutherland, R., and Greaves, M. (1981) *J. Exp. Med.* **153,** 726–731
12. Miyake, M., Koyama, M., Seno, M., and Ikeyama, S. (1991) *J. Exp. Med.* **174,** 1347–1354
13. Miyake, M., Nakano, K., Ieki, Y., Adachi, M., Huang, C. L., Itoi, S., Koh, T., and Taki, T. (1995) *Cancer Res.* **55,** 4127–4131
14. Higashiyama, S., Iwamoto, R., Goishi, K., Raab, G., Taniguchi, N., Klagsbrun, M., and Mekada, E. (1995) *J. Cell Biol.* **128,** 929–938
15. Schmidt, C., Kunemund, V., Wintergerst, E. S., Schmitz, B., and Schachner, M. (1996) *J. Neurosci. Res.* **43,** 12–31
16. Chen, M. S., Tung, K. S., Coonrod, S. A., Takahashi, Y., Bigler, D., Chang, A., Yamashita, Y., Kincade, P. W., Herr, J. C., and White, J. M. (1999) *Proc. Natl. Acad. Sci. U. S. A.* **96,** 11830–11835
17. Miyado, K., Yamada, G., Yamada, S., Hasuwa, H., Nakamura, Y., Ryu, F., Suzuki, K., Kosai, K., Inoue, K., Ogura, A., Okabe, M., and Mekada, E. (2000) *Science* **287,** 321–324
18. Le Naour, F., Rubinstein, E., Jasmin, C., Prenant, M., and Boucheix, C. (2000) *Science* **287,** 319–321
19. Wright, M. D., and Tomlinson, M. G. (1994) *Immunol. Today* **15,** 588–594
20. Maecker, H. T., Todd, S. C., and Levy, S. (1997) *FASEB J.* **11,** 428–442
21. Hemler, M. E., Mannion, B. A., and Berditchevski, F. (1996) *Biochim. Biophys. Acta* **1287,** 67–71
22. Rubinstein, E., Le Naour, F., Lagaudriere-Gesbert, C., Billard, M., Conjeaud, H., and Boucheix, C. (1996) *Eur. J. Immunol.* **26,** 2657–2665
23. Bradbury, L. E., Kansas, G. S., Levy, S., Evans, R. L., and Tedder, T. F. (1992) *J. Immunol.* **149,** 2841–2850
24. Takahashi, S., Doss, C., Levy, S., and Levy, R. (1990) *J. Immunol.* **145,** 2207–2213
25. Schick, M. R., and Levy, S. (1993) *J. Immunol.* **151,** 4090–4097
26. Imai, T., and Yoshie, O. (1993) *J. Immunol.* **151,** 6470–6481
27. Angelisova, P., Hilgert, I., and Horejsi, V. (1994) *Immunogenetics* **39,** 249–256
28. Szollosi, J., Horejsi, V., Bene, L., Angelisova, P., and Damjanovich, S. (1996) *J. Immunol.* **157,** 2939–2946
29. Berditchevski, F., Zutter, M. M., and Hemler, M. E. (1996) *Mol. Biol. Cell* **7,** 193–207
30. Mannion, B. A., Berditchevski, F., Kraeft, S. K., Chen, L. B., and Hemler, M. E. (1996) *J. Immunol.* **157,** 2039–2047
31. Matsumoto, A. K., Martin, D. R., Carter, R. H., Klickstein, L. B., Ahearn, J. M., and Fearon, D. T. (1993) *J. Exp. Med.* **178,** 1407–1417
32. Behr, S., and Schriever, F. (1995) *J. Exp. Med.* **182,** 1191–1199
33. Yanez-Mo, M., Alfranca, A., Cabanas, C., Marazuela, M., Tejedor, R., Ursa, M. A., Ashman, L. K., de Landazuri, M. O., and Sanchez-Madrid, F. (1998) *J. Cell Biol.* **141,** 791–804
34. Domanico, S. Z., Pelletier, A. J., Havran, W. L., and Quaranta, V. (1997) *Mol. Biol. Cell* **8,** 2253–2265
35. Berditchevski, F., and Odintsova, E. (1999) *J. Cell Biol.* **146,** 477–492
36. Skubitz, K. M., Campbell, K. D., and Skubitz, A. P. (2000) *FEBS Lett.* **469,** 52–56
37. Shevchenko, A., Keller, P., Scheiffele, P., Mann, M., and Simons, K. (1997) *Electrophoresis* **18,** 2591–2600
38. Yashiro-Ohtani, Y., Zhou, X. Y., Toyo-Oka, K., Tai, X. G., Park, C. S., Hamaoka, T., Abe, R., Miyake, K., and Fujiwara, H. (2000) *J. Immunol.* **164,** 1251–1259
39. Fitter, S., Sincock, P. M., Jolliffe, C. N., and Ashman, L. K. (1999) *Biochem. J.* **338,** 61–70
40. Sincock, P. M., Fitter, S., Parton, R. G., Berndt, M. C., Gamble, J. R., and Ashman, L. K. (1999) *J. Cell Sci.* **112,** 833–844
41. Radford, K. J., Thorne, R. F., and Hersey, P. (1996) *Biochem. Biophys. Res. Commun.* **222,** 13–18
42. Berditchevski, F., Bazzoni, G., and Hemler, M. E. (1995) *J. Biol. Chem.* **270,** 17784–17790
43. Levy, S., Todd, S. C., and Maecker, H. T. (1998) *Annu. Rev. Immunol.* **16,** 89–109
44. Horvath, G., Serru, V., Clay, D., Billard, M., Boucheix, C., and Rubinstein, E. (1998) *J. Biol. Chem.* **273,** 30537–30543
45. Imai, T., Kakizaki, M., Nishimura, M., and Yoshie, O. (1995) *J. Immunol.* **155,** 1229–1239
46. Orlicky, D. J., and Nordeen, S. K. (1996) *Prostaglandins Leukotrienes Essent. Fatty Acids* **55,** 261–268
47. Orlicky, D. J. (1996) *Prostaglandins Leukotrienes Essent. Fatty Acids* **54,** 247–259
48. Orlicky, D. J., Lieber, J. G., Morin, C. L., and Evans, R. M. (1998) *J. Lipid Res.* **39,** 1152–1161
49. Bergelson, J. M., St. John, N. F., Kawaguchi, S., Pasqualini, R., Berdichevsky, F., Hemler, M. E., and Finberg, R. W. (1994) *Cell Adhes. Commun.* **2,** 455–464
50. Weitzman, J. B., Pasqualini, R., Takada, Y., and Hemler, M. E. (1993) *J. Biol. Chem.* **268,** 8651–8657
51. Fukudome, K., Furuse, M., Imai, T., Nishimura, M., Takagi, S., Hinuma, Y., and Yoshie, O. (1992) *J. Virol.* **66,** 1394–1401
52. Pesando, J. M., Hoffman, P., and Conrad, T. (1986) *J. Immunol.* **136,** 2709–2714
53. Yauch, R. L., Berditchevski, F., Harler, M. B., Reichner, J., and Hemler, M. E. (1998) *Mol. Biol. Cell* **9,** 2751–2765

[4] X. A. Zhang and M. E. Hemler, unpublished data.

54. Serru, V., Le Naour, F., Billard, M., Azorsa, D. O., Lanza, F., Boucheix, C., and Rubinstein, E. (1999) *Biochem. J.* **340,** 103–111
55. DiPersio, C., Shah, S., and Hynes, R. (1995) *J. Cell Sci.* **108,** 2321–2336
56. Pleasure, S. J., Page, C., and Lee, V. M. (1992) *J. Neurosci.* **12,** 1802–1815
57. Brewer, G. J., Torricelli, J. R., Evege, E. K., and Price, P. J. (1993) *J. Neurosci. Res.* **35,** 567–576
58. Schaffner, W., and Weissmann, C. (1973) *Anal. Biochem.* **56,** 502–514
59. Chittum, H. S., Lane, W. S., Carlson, B. A., Roller, P. P., Lung, F. D., Lee, B. J., and Hatfield, D. L. (1998) *Biochemistry* **37,** 10866–10870
60. Eng, J. K., McCormick, A. L., and Yates, J. R. I. (1994) *J. Am. Soc. Mass Spectrom.* **5,** 976–989
61. Brown, D. A., and London, E. (1998) *Annu. Rev. Cell Dev. Biol.* **14,** 111–136
62. Simons, K., and Ikonen, E. (1997) *Nature* **387,** 569–572
63. Harder, T., Scheiffele, P., Verkade, P., and Simons, K. (1998) *J. Cell Biol.* **141,** 929–942
64. Claas, C., Stipp, C. S., and Hemler, M. E. (2001) *J. Biol. Chem.* **276,** in press
65. Green, J. M., Zhelesnyak, A., Chung, J., Lindberg, F. P., Sarfati, M., Frazier, W. A., and Brown, E. J. (1999) *J. Cell Biol.* **146,** 673–682
66. Krauss, K., and Altevogt, P. (1999) *J. Biol. Chem.* **274,** 36921–3697
67. Thorne, R. F., Marshall, J. F., Shafren, D. R., Gibson, P. G., Hart, I. R., and Burns, G. F. (2000) *J. Biol. Chem.* **275,** 35264–35275
68. Orlicky, D. J., Miller, G. J., and Evans, R. M. (1990) *Prostaglandins Leukotrienes Essent. Fatty Acids* **41,** 51–61
69. Indig, F. E., Diaz-Gonzalez, F., and Ginsberg, M. H. (1997) *Biochem. J.* **327,** 291–298
70. Seehafer, J. G., Tang, S. C., Slupsky, J. R., and Shaw, A. R. (1988) *Biochim. Biophys. Acta* **957,** 399–410
71. Seehafer, J. G., Slupsky, J. R., Tang, S. C., Masellis-Smith, A., and Shaw, A. R. (1990) *Biochim. Biophys. Acta* **1039,** 218–226